

CORE AND EDGE ELECTRON DYNAMICS DURING LOWER HYBRID CURRENT DRIVE EXPERIMENTS

Y. PEYSSON, M. GONICHE, R. ARSLANBEKOV, A. BÉCOULET, P. BIBET, A. CÔTÉ¹, C. CÔTÉ¹, Y. DEMERS¹, P. FROISSARD, V. FUCHS¹, P. GHENDRIH, A. GROSMAN, J. GUNN², D. GUILHEM, J.H. HARRIS³, J.T. HOGAN⁴, F. IMBEAUX, P. JACQUET¹, F. KAZARIAN, X. LITAUDON, J. MAILLOUX, D. MOREAU, V. PETRŽILKA⁵, R. PUGNO⁶, K.M. RANTAMÄKI⁷, G. REY, N. RICHARD¹, E. SÉBELIN, M. SHOUCRI¹.
Association EURATOM-CEA
CEA/Cadarache, 13108 Saint Paul-lez-Durance Cédex
France

Abstract

CORE AND EDGE ELECTRON DYNAMICS DURING LOWER HYBRID CURRENT DRIVE EXPERIMENTS

Characterisation of the core and edge fast electron dynamics during lower hybrid (LH) current drive experiments is a critical issue in view to achieve improved plasma performances by tailoring the current density profile in a steady state manner. At low power input ($P_{LH} = 2\text{MW}$), the localisation of the LH wave absorption exhibits a correlation with the radial position of the $q=1$ surface in the plasma, as deduced from magnetic measurements and equilibrium code predictions. Such an effect is observed either in stationary or transient conditions during LH assisted ramp-up experiments. The lack of LH power deposition in the core of the plasma is also confirmed by analysis of giant sawteeth in combined ICRH-LH scenarios. The implications of these results for theories of the LH wave dynamics in the plasma and current density profile control are discussed. LH power dissipation at the plasma edge, which may lead to anomalous heat loads on components magnetically connected to the radiating waveguide array is investigated theoretically and experimental data are compared to calculations. The key role played by the fraction of high- $n_{||}$ values of the LH wave power spectrum as well as the edge plasma density in the acceleration of thermal electrons is identified, and the possibility of an additional driving force is also discussed. The effect of the shape of the LH waveguide septa is analysed both theoretically and experimentally.

1. FAST ELECTRON DYNAMICS FROM BREMSSTRAHLUNG TOMOGRAPHY

The new hard x-ray (HXR) tomographic system which has been installed recently on TORE SUPRA with 59 lines-of-sight, and 8 energy channels between 20 and 200 keV for each chord, has allowed investigations of the LH wave dynamics at a level of accuracy which has never been reached so far on any tokamak [1]. Based on a robust *CdTe* technology [2], time and space resolutions of the diagnostic are respectively 4 ms and 5 cm, while the noise induced by neutron/ rays remains weak enough for a clear identification of the fast electron dynamics during operations with combined ion cyclotron resonance (ICRH) and LH heating, even at a very high input power level [2,3]. In these conditions, a detailed assessment of theories of the LH wave in tokamak plasmas may be performed, the cornerstone for a reliable control of the current density profile and achievement of steady-state negative core magnetic shear by LH means in high power plasmas [3].

¹ Centre Canadien de Fusion Magnétique, Varennes, Québec, J3X 1S1, Canada

² MPB Technologies inc. Pointe-Claire, Québec, Canada

³ Australian National University, Canberra, ACT0200, Australia

⁴ Oak Ridge National laboratory, Oak Ridge, Tennessee, USA

⁵ Institut of Plasma Physics, 182 21 Praha 8, Czech Republic

⁶ Consorzio RFX, IGI Padova, 4 Corsi Stati Uniti, Padova, Italy

⁷ Association EURATOM-TEKES, Espoo, Finland

Recent investigations have been carried out at fairly high plasma current values ($I_p \approx 0.6$ MA) and moderate input LH power levels ($P_{LH} \approx 2.5$ MW), in view to extend former studies of LH-sustained magnetic shear reversal to nominal operating conditions of TORE SUPRA [4]. Since the fraction of current driven by the LH wave remains at a low level, the resulting perturbation of the plasma equilibrium may be almost neglected. This condition is important in order to avoid large non-linear effects which result from the coupling between the LH wave dynamics and plasma equilibrium. In experiments addressed in this paper, the value at which the launched LH power spectrum is peaked ranges between $n_{//peak} = 1.8$ and 2.2, with a full width of 0.4. However, since the LH power deposition profiles are very weakly dependent of the waveguide phasing but of the strong toroidal upshifts and downshifts, as observed experimentally, variations of this parameter is not critical for the following analysis. Core electron density ranges between 2.0 and $3.0 \times 10^{19} \text{ m}^{-3}$. As shown in Fig. 1, the non-thermal HXR emission profiles between 60 and 80 keV is quite systematically hollow, and the peak position $\rho_{HXRpeak(60-80keV)}$ shifts towards the plasma edge as far as the plasma current increases. This evolution, which has been already reported with the former HXR diagnostic [5], is confirmed by a current scan between 0.6 and 1.6 MA in stationary conditions, but also in time-dependent conditions during LH-assisted ramp-up experiments. An illustration of such an effect is given in Figs. 2 and 3 for a transient regime, where main traces of a representative shot are reported, as well as line-integrated and Abel inverted local HXR emissions between 60 and 80 keV at different time steps. The consistency between data obtained with both cameras, and the direct evidence of hollowness from raw data make the determination of the peak position very robust, even if time integration is short (8 ms). In the early phase of all LH-assisted ramp-up discharges, the HXR emission is narrow and strongly peaked at all photon energies. As far as plasma current increases, HXR profiles broaden progressively until a smooth transition to

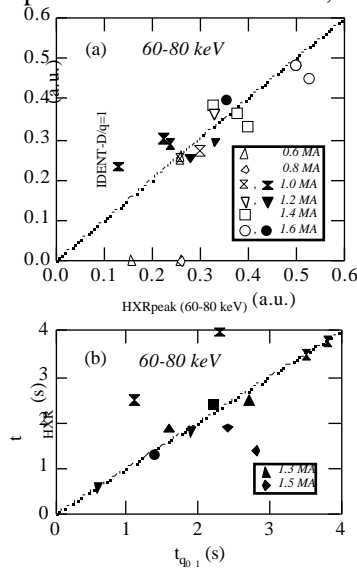


Fig. 1: (a) Peak position of the HXR profile at 60-80 keV vs. location of $q=1$ predicted by IDENT-D code for ramp-up experiments (black points) and stationary conditions (white points) at different plasma currents. (b) Time of transition to hollow HXR profiles vs. time of occurrence of $q = 1$ surface in the plasma from polarimetry measurements.

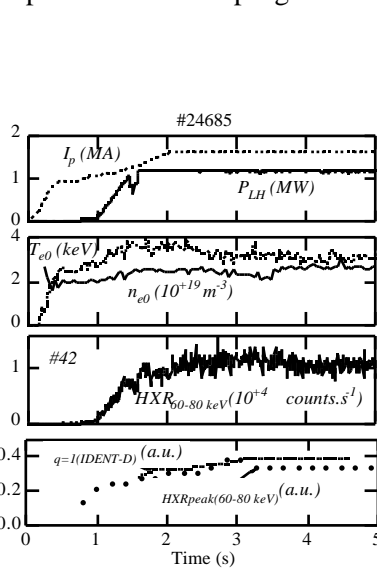


Fig. 2: Time variations of the plasma current, LH power, central electron temperature and density, line-integrated HXR emission (central chord #42, vertical camera) between 60 and 80 keV, and evolutions of the positions of the HXR off-axis peak and $q=1$ surface predicted by IDENT-D code, for the LH assisted ramp-up discharge number #24685.

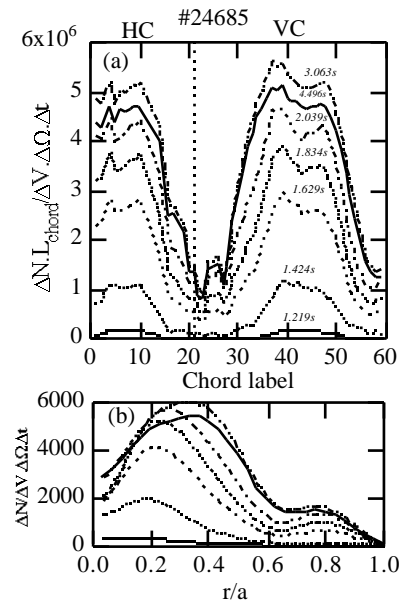


Fig. 3: (a) Line-integrated HXR signals between 60 and 80 keV, for the horizontal (HC) and vertical (VC) cameras at different time steps (discharge #24685). (b) Abel inverted local HXR emission as deduced from line-integrated measurements displayed in Fig. 3a. Each type of line corresponds to the time indicated above in Fig. 3a.

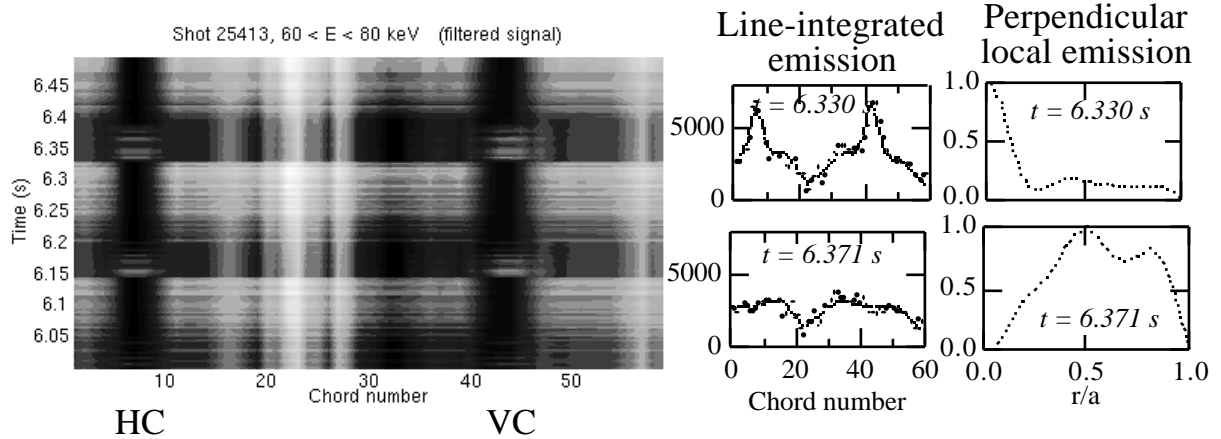


Fig. 4: Line-integrated HXR emission for all chords as a function of time, between 60-80 keV during combined ICRH-LH discharge. The black color corresponds to a high HXR emission, while the white one to weak emission. The direct evidence of hollowness from line-integrated measurements is observed on both cameras. Details of the line-integrated and Abel inverted local emission profiles are given for two different time steps. The pedestal in the line integrated emission, which arises from LH wave current drive is insensitive to the sawtooth perturbation.

hollow profiles occurs, while electron temperature and density but also main plasma parameters remain at a constant level throughout the discharge (Fig. 2). Time at which this transition takes place exhibits a correlation with the occurrence of $q_0 = 1$ in the plasma, as deduced from polarimetry measurements for a large number of shots (Fig. 1b). Such an evidence is sustained by equilibrium calculations carried out with the IDENT-D code [6]. Both in stationary and transient conditions, the localization of the observed HXR off-axis peak is close to the radial position of the predicted $q = 1$ surface, either for several different discharges (Fig. 1), or at successive time steps for the same shot (Fig.2). Times at which small electron temperature sawteeth become visible coincide roughly with transitions towards hollow HXR profiles, while the inversion radius is consistent with the position of the $q = 1$ surface within the experimental uncertainty.

The fact that stationary HXR profiles are established on a very short time scale (~ 4 ms) when the LH power is applied several seconds after the onset of the plateau of the plasma current, while they evolve on a resistive time scale (0.2-0.4 s) during the ramp-up gives strong evidence of the key role played by the current density profile on the LH power deposition. Moreover, the sustainment of hollow HXR profiles in stationary conditions confirms the very weak diffusion rate of non-thermal electrons, a result which has been already suggested by numerous LH experiments, but in a far less clear manner [7].

The lack of LH power deposition in the core of the plasma when $q_0 = 1$ is also observed directly from a time-space analysis of giant sawteeth during combined ICRH-LH experiments. In the case here presented, up to 6 MW of ICRH power is coupled to the plasma in the minority heating scheme. The core electron temperature reaches $T_{e0} = 5.5$ keV approximately, and the period of the large saturated sawteeth is about 200 ms. The HXR signals recorded by central chords in the first three photon energy channels (20-40, 40-60 and 60-80 keV) exhibit all sawtooth modulations. From a detailed analysis, it turns out that even in the interval 60-80 keV, the thermal contribution is non-negligible in the center as compared to the non-thermal one, except after a sawtooth crash. For more off-axis chords however, the suprathermal emission always dominates, and no sawtooth modulations are observed. As shown in Fig. 4, the sawtooth crash leads to a strong modification of the HXR profile emission between 60-80 keV, which becomes strongly hollow. The time sequence indicates that hollowness remains during more than 40 ms, much larger than the fast electron acceleration time scale by the wave electric field (~ 1 ms). This analysis confirms quite directly that LH power deposition is hollow when the $q = 1$ surface is inside the plasma, in agreement with the previous experiments with LH power only. Moreover, the off-axis power deposition of the LH wave is clearly insensitive to the sawtooth crash. Such a result is consistent with the decrease of the relative amplitude of the sawteeth with the photon energy

which is observed systematically whatever the type of sawtooth activity, when the fraction of LH power launched in the plasma is larger, as compared to the ICRH one [2].

The role played by the $q = 1$ surface in the LH wave dynamics which is observed experimentally raises several questions concerning the modelisation of the LH wave dynamics, and its ability to be used for tailoring the current density profile in the plasma. From recent electron cyclotron resonance heating (ECRH) experiments [8], it turns out that transport barriers are observed at all rational q -surfaces, which strongly affect electron temperature profiles. A similar effect may append with the LH wave but, since power absorption is much broader, only the contribution of $q = 1$ can be identified. Even if the exact position of the $q = 1$ surface is usually subject to large uncertainties, especially during LH experiments where no or weak sawtooth activity is detected, the parametric dependence which is observed gives strong confidence that details of the magnetic topology have a large effect on the LH power absorption. Refined experiments have to be carried out, in view to identify pertinent ingredients that have to be considered in an LH wave model, for an accurate description of the experimental phenomenology at all plasma current values.

2. LH POWER DISSIPATION AT THE PLASMA EDGE

During LH current drive experiments on various tokamaks (ASDEX, TORE SUPRA, TdeV), anomalous heat loads are observed on components magnetically connected to the radiating lower hybrid waveguide array. On TdeV, a large asymmetry in the power deposition on the divertor plates is measured [9], and by changing the safety factor q , it is assessed that this anomalous heat flux is related to particles flowing along the field lines from the grill to the magnetically connected plates. On TORE SUPRA [10], localised hot spots are detected on several components magnetically connected on either side of the LH grills, both in the limiter and the ergodic divertor configuration. Several experimental observations using x-ray detectors and Langmuir probes indicate that heat flux is mainly carried by fast electrons generated in front of the grill, whose energy lies between 100 eV and 5 keV approximately.

An analysis of the heat flux is performed on TORE SUPRA by infra-red (IR) thermography. The high resolution of the camera (2mm) allows to characterise the geometric dimensions of the hot spots. In the poloidal direction, the hot spots are spaced with the same periodicity as the row of waveguides and have a typical size of 3-4 cm. This pattern is similar to the RF electric field distribution at the grill mouth. The radial extension of the flux tube carrying these fast electrons is measured by two methods. The power deposition profile on a neutraliser of the ergodic divertor is derived from the IR imaging. Taking into account the grazing angle of the field lines obtained from the field line tracing code MASTOC [11], it is deduced that the radial width, defined as the width at mid-height of the profile, is 5-6 mm [12]. This result is confirmed by shadowing one grill with the other in the limiter configuration. The first grill is launching RF power (1.2 MW) and its heat flux on a plasma facing component intercepting these fast particles is measured. The second grill, located toroidally between the first grill and the intercepting component is moved forward from shot to shot. When the grill number two is 6 mm ahead of the first grill, a decrease of the heat flux by a factor 2 is observed. At the same time the heat load on the second grill increases consistently. The limited radial extension of this particle beam allows a control of the power deposition location. Recently, the protruding length of the guard limiters of one of the TORE SUPRA LH grill has been increased from 1.5 mm to 6 mm. Preliminary results tend to confirm that the additional heat flux on this guard limiter increase significantly as expected.

The LH power dependence is also investigated on TORE SUPRA from the IR images. It is observed that the heat flux on a limiter, connected to the grills with a 20m connection length, increases more rapidly than the launched LH power, as shown in Fig.5. Further experiments demonstrate moreover that this heat flux is related not only to the LH power level, but also to the electronic density in front of the grills. On TdeV, calorimetric measurements of the secondary divertor plates, which are only connected to the scrape-off layer (SOL), indicate that the deposited power varies almost linearly with the edge density. On TORE SUPRA, this linear dependence is confirmed by IR thermal analysis of the neutraliser plates of the ergodic divertor. Because of this SOL density dependence, heat fluxes in the range of 8-15 MW/m² have been

measured when the edge density $n_{e,edge}$ is around $2 \times 10^{18} \text{ m}^{-3}$. It is concluded that an optimisation of the position of the LH grills is required in order to maintain a good wave coupling and moderate heat fluxes ($< 5 \text{ MW/m}^2$). In this case, the total power dissipated in the edge is below 3% of the LH injected power.

The fast electron generation process in front of the LH grill is investigated theoretically. For current drive experiments, the antenna excites a wave spectrum with a high directivity: most of the power ($\sim 70\%$) is launched with a low parallel refraction index ($n_{\parallel} \sim 2$). However the launched n_{\parallel} power spectrum is rich in harmonics and in particular, lines at very high n_{\parallel} ($|n_{\parallel}| > 25$) carry a sufficient fraction of power (2-3 %) to resonantly accelerate thermal edge electrons ($\sim 20 \text{ eV}$). As these electrons gain velocity, they can interact with lower and lower n_{\parallel} values up to a threshold given by vanishing overlap of the spectrum Fourier modes. For typical antenna electrical field strengths (3kV/cm), electrons can be accelerated up to a few keV [13]. The motion of electrons in the near field approximation is calculated from a simplified 1D model [10,13]. Particles are launched at one end of the grill and the velocity is calculated step by step after each transit from one waveguide to another. Starting from a thermal velocity distribution, it is found that, for typical electric field strength (2-5 kV/cm), electrons are accelerated up to 1-5 keV, with an average value in the hundreds of eV range.

Calculations for Tore Supra plasma shots in which the LH power varies from 1.1 to 3.2 MW, shows that the mean energy of the accelerated electrons scales with the averaged electric field E_{RF} as $E_{RF}^{3/2}$ and varies for these shots between 280 and 640eV. In order to compute the heat flux, a modelling of the interaction of the accelerated electrons with the guard limiter of one of the Tore Supra antenna is carried out. Because of the sheath effect, the heat flux normalized to the convective flux F_0 rises to a maximum for a fast electron ratio near 2% and decreases weakly for higher ratios. With such a ratio, a rather good agreement between the calculated and measured heat fluxes is obtained (Fig.6).

An electrostatic particle-in-cell model is also developed [14]. This model, which is two-dimensional in space and three-dimensional in velocity, allows to calculate self-consistently the electric field level. Using this code, one can also demonstrate the possible generation of a fast tail in the velocity distribution. For an injected power density of 48 MW/m^2 , calculations give a maximum energy of about 2 keV for the fast electron population. Furthermore, these simulations allow to evaluate the fraction of absorbed LH power and the radial LH power deposition profile. The fraction of absorbed power ($\sim 3\%$) is quite consistent with measurements, at least in the low edge density case but the absorption length is found to be shorter ($\sim 1 \text{ mm}$) than the experimental value. This result is expected since most of the high spatial harmonics of the LH wave are strongly absorbed by Landau damping. Therefore, they can only propagate in a few mm narrow

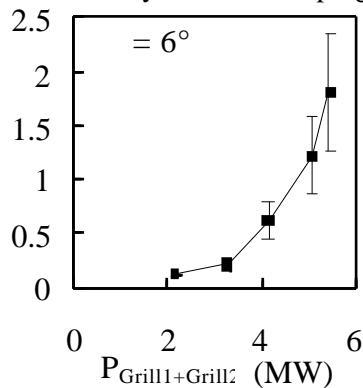


Fig.5. Anomalous heat flux on a limiter magnetically connected to the 2 LH grills vs. total LH power ($I_p=1 \text{ MA}$, $\langle n_e \rangle = 2.0 \times 10^{19} \text{ m}^{-3}$).

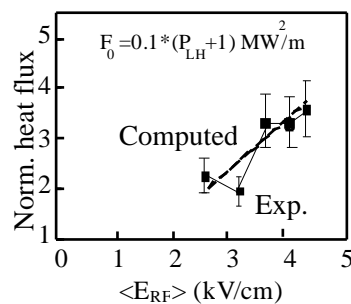


Fig.6. Experimental (solid line) and computed (dashed line) heat fluxes on a LH line guard limiter. ($I_p=1 \text{ MA}$, $\langle n_e \rangle = 2 \times 10^{19} \text{ m}^{-3}$, $P_{LH}=1.1-3.2 \text{ MW}$ - $n_{fast}/n_{th}=2\%$)

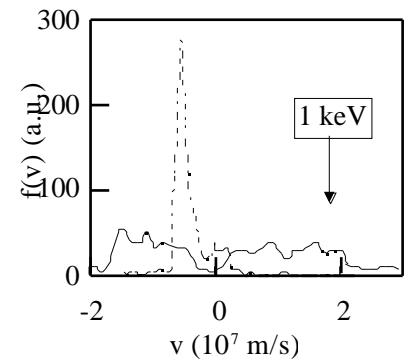


Fig.7. Velocity distribution without random fields (dashed line) and with random fields (solid line).

layer in front of the LH grill. The electron acceleration by the launched field is thus limited to this very narrow domain. However, higher order modes may be again spontaneously excited by the nonlinear LH wave scattering on selfconsistent ponderomotive density perturbations in a much wider layer [15], having a width of few cm. Other spontaneously excited random fields may arise from the LH wave scattering on plasma density fluctuations, or because of parametric processes. The enhancement of the electron acceleration by these spontaneously excited random fields, and the resulting enlargement of the width of the acceleration layer is illustrated in Fig. 7. For the computations, the number of launched higher modes is chosen to 5, in order to model the wider layer several mm radially beyond the very narrow layer at the grill mouth.

The key role of the high- n_{\parallel} content of the spectrum in the acceleration process is well established, both experimentally and theoretically. This offers a number of possibilities of reducing the associated anomalous heat flow through modification of the spectrum. In particular, the high- n_{\parallel} spectrum content can be reduced by rounding off the waveguide septa edges. On TdeV the septa of the upper antenna row were rounded off, while the septa of the lower row were kept with sharp angles. A comparison between the two rows is made for similar LH density power and for same edge plasma densities. The two rows had the same reflection coefficient. At low density ($\langle n_e \rangle = 3.5 \times 10^{19} \text{ m}^{-3}$, $n_{e,edge} = 0.7 \times 10^{18} \text{ m}^{-3}$), it is found that the power dissipated in front of the row with rounded septa is reduced by approximately 20 % which compares favourably with 30 % predicted by calculation [16]. However at high edge density ($\langle n_e \rangle = 5 \times 10^{19} \text{ m}^{-3}$, $n_{e,edge} = 1.5 \times 10^{18} \text{ m}^{-3}$), there is no significant reduction of the power dissipation with rounded septa, suggesting that Landau damping of waves in front of the grill could be enhanced by other mechanisms. For an ITER type antenna, with thicker plates, numerical results indicate that electron acceleration will disappear with rounded septa.

ACKNOWLEDGEMENTS

The support on the hard x-ray tomographic system by the TORE SUPRA technical staff and L. DELPECH is greatly acknowledged. The staffs of TORE SUPRA and TdeV tokamaks who give support to run all the LH experiments are gratefully acknowledged.

REFERENCES

- [1] Y. Peysson, et al, *Proc. of the 24th Eur. Phys. Soc. Conf. on Control. Fusion and Plasma Physics*, Berchtesgaden, **21A**, part I (1997) 229.
- [2] Y. Peysson and R. Arslanbekov, *Nucl. Instr. and Methods*, **380** (1996) 423.
- [3] T. S. Taylor, *Plasma Phys. Control. Fusion*, **39** (1997) B47.
- [4] X. Litaudon et al., *Plasma Phys. Control. Fusion*, **38** (1996) 1603.
- [5] Y. Peysson et al. *Phys. Plasmas*, **3** (1996) 3668.
- [6] E. Joffrin et al, *Proc. of the 22th Eur. Phys. Soc. Conf. on Control. Fusion and Plasma Physics*, Bornemouth, **19C**, part IV (1995) 125.
- [7] Y. Peysson, *Plasma Phys. Control. Fusion*, **35** (1993) B253.
- [8] N.J. Lopes Cardozo et al., *Plasma Phys. Control. Fusion*, **36** (1994) 133.
- [9] J.Mailloux et al, *J.Nuc.Materials*, **241-243** (1997) 745.
- [10] M.Goniche et al., *Nuclear Fusion*, **38** (1998) 919.
- [11] Ph.Ghendrih and A.Grosman, *J.of Nucl.Mat.*,241-243 (1997) 517
- [12] R.Pugno et al., *13th Int.Conf. on Plasma Surface Interactions in Controlled Fusion Devices, San Diego, to be published in J.Nucl.Materials* (1998).
- [13] V.Fuchs et al., *Phys.Plasmas* , **3** (1996) 4023.
- [14] K.M.Rantamäki et al., *Proc.of the 2nd Europhysics Top.Conf. on RF Heating and Current Drive of Fusion Devices*, Brussels, **22A** (1998) 173.
- [15] V. Petrzilka: *Plasma Phys. Contr. Fusion*, **33** (1991) 365.
- [16] P. Jacquet, et al. *Effects of septa shape and plasma density on electric field spectra of LH antennas*, CCFM report, CCFM-RI-474e (1997).